Study Report

SR472 [2023]

Performance of magnesium oxide (MgO) boards in New Zealand

Anna Walsh

BRANZ
1222 Moonshine Rd, RD1, Porirua 5381
Private Bag 50 908, Porirua 5240
New Zealand
branz.nz

ISSN: 1179-6197

Preface

This report has been prepared as part of the BRANZ research project QR11765 *Performance of magnesium oxide (MgO) boards*. This report presents the findings of a series of experiments on different MgO-based boards that are available for use in New Zealand.

Acknowledgements

This work was funded by the Building Research Levy.

Performance of magnesium oxide (MgO) boards in New Zealand

BRANZ Study Report SR472

Authors

Anna Walsh

Reference

Walsh, A. (2023). *Performance of magnesium oxide (MgO) boards in New Zealand.* BRANZ Study Report SR472. Judgeford, New Zealand: BRANZ Ltd.

Abstract

Magnesium oxide (MgO) boards are a relatively new material to the construction industry, both in New Zealand and internationally. MgO boards are used as an alternative to traditional sheet materials such as those made with fibre-cement and gypsum. In New Zealand, there are examples of MgO boards used in both interior and exterior applications, including as sheathing, internal linings, rigid wall underlays and cladding, and as components of prefabricated building systems such as structural insulated panels (SIPs). MgO boards have received attention in the last decade due to reported failures of building systems where these boards have been a component, and subsequent research has identified variability in the performance of boards made with different compositions. This study investigated the chemical and physical properties of four MgO boards available in New Zealand under a range of exposure conditions. The aim of the study was to identify whether there was any variability in the performance of boards from different suppliers. Overall, the findings from this study show that there is variability between how MgO boards from different suppliers perform under New Zealand conditions. Variability in performance is related to variability in composition. The results highlight the importance of considering the likely in-service conditions when assessing the suitability of a given MgO board for a given application.

Keywords

Magnesium oxide, MgO.

Contents

Figures

Tables

1. Introduction

Magnesium oxide (MgO) boards are a relatively new material to the construction industry both in New Zealand and internationally. 'MgO board' is typically an umbrella term used to refer to boards made from an MgO cement, of which there are different varieties. MgO boards are used as an alternative to traditional sheet materials such as those made with fibre-cement and gypsum. In New Zealand, there are examples of MgO boards used in both interior and exterior applications, including as sheathing, internal linings, rigid wall underlays and cladding, and as components of prefabricated building systems such as structural insulated panels (SIPs).

The reported benefits of MgO boards typically relate to fire resistance, low density and availability. These characteristics have seen use of MgO boards increase, particularly for lightweight construction systems, both in New Zealand and internationally. However, as the use of this material increases, issues with how some MgO board products perform in reaction to moisture have become apparent. MgO boards have received attention in the last decade due to failures of building systems where these boards have been a component. In 2015, the performance of MgO board used as a cladding material in Denmark triggered much of the research in this area. In the Danish example, MgO board had been widely used since 2010 as part of ventilated façades for new or renovated Danish buildings. Several problems began to appear in 2014, which were reportedly related to moisture absorption and corrosion of fasteners and metal components attached to the MgO board (Rode, Bunch-Nielsen, Hansen & Grelk, 2017).

Failures related to the use of MgO board have more recently been reported in other locations such as Australia and New Zealand. Research by Jays, Olofinjana and Young (2019) investigated the performance of several MgO boards used for cladding in Australia. Aiken, Russell, McPolin and Bagnall (2020) looked at potential performance variability of boards with different chemical compositions. Key findings have been that MgO boards produced by different manufacturers can exhibit differences in both their physical and chemical characteristics, including how they perform when exposed to high relative humidity conditions (Jays et al., 2019; Aiken, Russell et al., 2020). Some of the boards tested in the study showed behaviour like that seen in Denmark, whereas others showed no deterioration after exposure to high humidity conditions for 60 weeks (Aiken, Russell et al., 2020).

Performance variations between MgO boards from different suppliers was one consequence of there being no widely accepted way to test or verify the consistency of MgO boards through standardisation. The International Code Council Evaluation Service (ICC-ES) developed AC386 *Acceptance criteria for fiber-reinforced magnesium-oxide-based sheets.* AC386 provides a means for MgO boards used as interior substrate sheets to be recognised in an ICC-ES evaluation report under the US-based building codes. To the best of our knowledge, one MgO board supplier in New Zealand has tested their product to AC386. However, this is not a requirement in New Zealand and does not guarantee product compliance with the New Zealand Building Code. In the UK, work to develop a publicly available specification (PAS) for MgO board use in buildings was initiated in May 2020 by the British Standards Institute (BSI) in conjunction with the MgO Building Board Trade Association (MOBBTA). The final document, PAS 670:2021 *Magnesium oxide-based boards for use in buildings – specification,* is intended to support improved quality assurance of MgO boards in the UK.

As mentioned above, the term 'MgO board' typically refers to boards made from an MgO-based cement, namely magnesium oxychloride (MOC) and magnesium oxysulphate (MOS). MOC and MOS cements are formed by a reaction between MgO powder with either magnesium chloride ($MgCl_2$) or magnesium sulphate ($MgSO_4$) solutions, respectively. To produce an MgO board, the cement component is combined with filler materials such as wood and perlite and a reinforcing mesh layer (Figure 1). Materials and numbers of layers may differ between boards from different manufacturers.

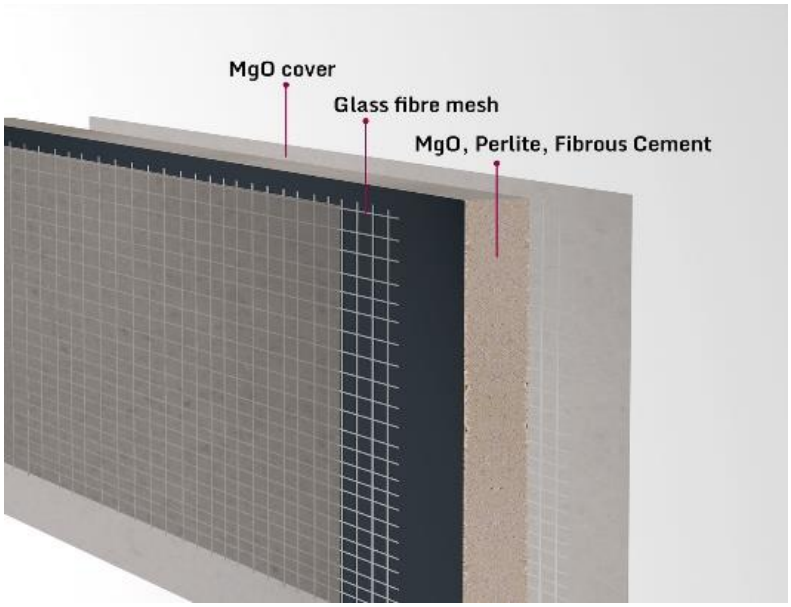

Figure 1. Structure of a typical MgO board.

MgO powder is obtained from the extraction of magnesium carbonate ($MgCO_3$ or magnesite) and subsequent calcination at temperatures between 600–1,300°C (Walling & Provis, 2016). The calcination temperature is cited as a reason that MgO boards have favourable environmental properties compared to Portland cements, which require calcination at temperatures more than 1400°C (Wang, Chen, Tsang, Poon & Shih, 2016).

Because of its hygroscopic nature, some MOC boards have been found to be unsuitable for use in high-humidity environments. Rode et al. (2017) found that, at relative humidity conditions above 85%, droplets of salty water formed on the surface of MOC samples. Similarly, Jays et al. (2019) determined that high chloride concentrations in MOC boards made them prone to absorbing water at high relative humidity conditions and could lead to chloride-containing leachate. Chloride leachate was found to attack non-stainless steel fasteners, and the formation of 'teardrops' on the board surface was found to cause issues even in the absence of ferrous fasteners (Jays et al., 2019).

The bending strength and water absorption properties of MOC and MOS boards were compared to those of fibre-cement, gypsum plasterboards and wood-based boards and were found to be comparable. Both MOC and MOS boards performed better than gypsum plasterboard and wood-based boards during exposure to soak-dry and freeze-thaw cycles and were comparable to fibre-cement boards, with strength losses of less than 13% observed (Aiken, McPolin, Russell, Madden & Bagnall, 2020). In the same study, MOS samples saw significant expansion in the moisture movement test (~0.16%) whereas MOC samples expanded less (~0.06%), suggesting that MOC boards have better resistance to expansion than MOS boards.

Composition analysis by X-ray diffraction (XRD) showed that the main product in MOC boards is the magnesium chloride hydroxide hydrate 5 $Mg(OH)_2$. $MgCl_2$. $8H_2O$, known as "5-phase", which has been reported as the preferable phase for structural applications due to its mechanical properties. Other phases can be formed in MOC cements depending on the curing temperature and molar ratios used to manufacture the product (Aiken, McPolin et al., 2020). In an investigation into the teardrop formation phenomenon observed in MgO boards used in Danish facades, Aiken, McPolin et al. (2020) found that accelerated ageing caused decomposition and dissolution of 5-phase magnesium chloride hydroxide hydrate. This decomposition resulted in a chloride-rich solution being free to leave the boards and present as teardrops (or 'crying').

As a result of the failures related to the use of MOC boards in Denmark, Wøhler Neilsen et al. (2019) compared the properties of MOC and MOS boards used as sheathing in exterior walls. The study investigated the chemical composition, reaction-to-moisture properties and effect of different relative humidity conditions on MOS boards at two thicknesses (9 mm and 12 mm) and an MOC board (12 mm). The study concluded that both types of board absorbed unacceptable amounts of water from a humid environment but that MOS boards condensed less water from the environment than MOC when exposed to high relative humidity.

MgO board has a relatively short history of use internationally, and information is needed to better assess its suitability for use in different applications. The purpose of the research described in this report was to identify any potential performance differences between different MgO boards available for use in New Zealand.

2. Materials

Four different MgO boards were selected as representative of the products available in New Zealand. These boards were sourced from commercial suppliers and included in the test programme.

Throughout this report, all data are presented anonymously and specimens are denoted as described in Table 1.

Table 1. Specimen codes and descriptions.

Specimen code	Description
MgO1	Magnesium oxide board
MgO2	Magnesium oxide board
MgO3	Magnesium oxide board
MgO4	Magnesium oxide board

3. Methods

MgO boards have typically been used as an alternative to fibre-cement sheets in internal and external building applications.

There is currently no standard available for assessing MgO boards for their suitability to the New Zealand context so test methods were selected based on those for similar products and those used in similar studies of MgO performance. The tests were based on those used in studies on MgO board from both the UK and Australia (Aiken, McPolin et al., 2020; Jays et al., 2019), as well as the type-tests included in AS/NZS 2908.2:2000 commonly used to assess the suitability of fibre-cement sheets for use in New Zealand. Detailed results are provided in Appendix A.

3.1 Composition analysis

The elemental composition of MgO samples was determined using X-ray fluorescence spectrometry (XRF). Samples of MgO board were prepared for analysis using two methods. In the first method, samples were ignited at 1,000°C and fused into glass beads with lithium tetraborate. The second method involved grinding samples into a homogeneous powder that was analysed in its entirety at oven dried (110°C) weight.

3.2 Modulus of rupture (MOR)

Modulus of rupture (MOR), or bending strength, is a routinely specified mechanical property used for the grading of cellulose fibre-cement sheet products. MOR was determined in accordance with clause 8.1.2.1 of AS/NZS 2908.2:2000 *Cellulose-cement products – Flat sheets* using 250 x 250 mm square specimens. Testing was conducted with an Instron universal testing machine equipped with a calibrated 10 kN load cell and Bluehill control software. A three-point bending apparatus was employed for loading with a support span of 215 mm and a constant crosshead deflection rate of 25 mm/min.

Due to the anisotropy typically observed in fibre-cement composites, testing was carried out both parallel to (machine direction) and perpendicular with (cross direction) the dominant orientation of the fibre.

The individual MOR of a specimen in MPa is calculated as follows:

$$R_f = \frac{3Pl}{2be^2}$$

where:

Rf is the modulus of rupture (MPa)

P is the breaking load (N)

l is the distance between the support axes (215 mm)

b is the width of the test piece (250 mm)

e is the average thickness of the test specimen at the break.

The MOR of a sheet is defined in clause 8.1.2.1.7 of AS/NZS 2908.2:2000 as the "arithmetic mean of the four values (two values in each direction)".

MOR specimens were preconditioned by soaking in water at ambient laboratory temperature for 24 hours before testing in a saturated surface-dry state.

For reference, the MOR was also determined for the sheets at equilibrium moisture content (EMC), which was achieved by preconditioning the test specimens for 7 days in a controlled environment room maintained at 23 ± 2°C and 50 ± 5% relative humidity (RH).

3.3 Frost resistance

Frost resistance testing was carried out in accordance with clause 8.2.3 of AS/NZS 2908.2:2000. Standard 250 mm square MOR specimens were prepared in pairs with the corresponding wet bending strength specimens described in the previous section. The latter served as controls to allow any loss in performance on exposure to the freezing conditions to be quantified.

The test specimens were subjected to 50 freeze-thaw cycles consisting of repeated cooling to -20 ± 2°C followed by thawing in water to reach +20 ± 2°C, as specified by clause 8.2.3.3 of AS/NZS 2908.2:2000. A single freeze-thaw cycle was completed in 4 hours, with the specified temperature extremes maintained for 1 hour. Prior to commencement of temperature cycling, the specimens were immersed in water at 5°C until constant mass was achieved, defined as < 0.5% difference over consecutive weighings at 24-hour intervals. At this point, the specimens were sealed into heavy-gauge polythene bags to maintain their water-saturated condition through the duration of the test. At the conclusion of cycling, the specimens were reconditioned under ambient laboratory conditions for 7 days and then visually examined for any defects.

The susceptibility of the samples subjected to freeze-thaw damage was quantified by comparing the average MOR in the wet condition of the temperature-cycled test pieces with the strength of pairs of control specimens cut from the corresponding as-received board.

3.4 Warm water immersion

Warm water soaking evaluates the potential for degradation of the cellulose fibre by alkali leaching from the cement matrix, changes in the nature of the fibre bonding or potential unsoundness in the composition of the cement.

Pairs of specimens cut from each of five test sheets were continuously immersed in hot water at 60 ± 2°C for 56 days, in accordance with clause 8.2.4 of AS/NZS 2908.2:2000, before determining their wet condition MOR. As with freeze-thaw testing, any deterioration in performance was evaluated by comparing the wet condition MOR of the test specimens with corresponding values for the as-received sample.

3.5 Soak-dry

This test assesses the susceptibility of boards to deterioration due to dimensional changes caused by soak-dry exposure. During natural weathering, the fibre content of fibre-cement boards can be exposed to repeated wetting and drying cycles, causing alternate swelling and shrinkage with the potential to break down the fibre or disrupt the fibre-matrix bond.

Soak-dry testing was carried out in accordance with clause 8.2.5 of AS/NZS 2908.2:2000, which submits pairs of standard MOR specimens cut from each of the

five test sheets to 25 cycles of drying in a ventilated oven at 60 ± 5°C and RH < 20% for 6 hours followed by immersion in water at ambient laboratory temperature for 18 hours. The performance of the test specimens after the 25 cycles was evaluated by comparing their MOR in the wet condition with the corresponding values for the as-received board.

3.6 Water vapour transmission

This test was carried out following the water method in ASTM E96/E96M-13 *Standard test methods for water vapor transmission of materials*. Three 90 mm discs were cut from each of the four MgO boards. Each disc was mounted in a specimen dish containing deionised water and sealed around the perimeter. A single control sample containing no water but otherwise identical to the test samples was prepared and placed in controlled laboratory conditions of 23 ± 2°C and 50 ± 5% RH during the test. The control was used to tare the balance before each weighing. The tests were carried out over a period of up to 19 days once the rate of mass loss of the control sample had lowered.

3.7 Water absorption

This test was carried out following the method described in section 9 of ASTM C1185-08 *Standard test methods for sampling and testing non-asbestos fiber-cement flat sheet, roofing and siding shingles, and clapboards*. Specimens of 100 x 100 mm were dried to constant weight in an oven at 90°C and then cooled at room temperature in a desiccator. The dry weight of each specimen was recorded. Specimens were then submerged in clean water at 23 ± 4°C for 48 hours and 35 minutes, after which they were wiped with a damp cloth and weighed. The water absorption value for each specimen was calculated as follows:

$$water\ absorption, mass\ \% = \left[\frac{Ws - Wd}{Wd}\right] \times 100$$

where:

Ws is the saturated mass (g) of specimen

Wd is the dry mass (g) of specimen.

3.8 Performance in a high-humidity environment

This test was carried out based on the method described in section 13.2 of PAS 670:2021. Specimens with dimensions 250 x 250 mm were conditioned in a laboratory environment until constant mass was reached. Conditioned samples were placed on a vertical rack and into a climate chamber at a temperature of 30 ± 2°C and 90% RH for 90 days. Following completion of the humidity test, samples were reconditioned and tested for MOR in accordance with clause 8.1.2.1 of AS/NZS 2908.2:2000.

A separate test was conducted to monitor for water droplet formation on the surface of MgO samples during exposure to 90% RH. For this test, four specimens of 90 x 90 mm were attached to the underside of plastic container lids. The containers had two holes of 10 mm diameter drilled into each side of the box so that the internal conditions would match that of the climate chamber (30 ± 2°C and 90% RH). Visual observations were made regularly throughout the 90-day test period to monitor for water droplet formation.

3.9 Fastener corrosion

Two strips were cut from each MgO sample with dimensions 300 x 40 mm and 300 x 60 mm respectively, and five fasteners with different coatings were inserted into each strip. Fasteners were sourced from Otter, and their characteristics are given in Table 2.

Table 2. Fasteners used in corrosion analysis.

Designation	Fastener coating description	Size
A	316 stainless steel	10 g x 50 mm
B	304 stainless steel	8 g x 32 mm
C	Mechanically plated	8 g x 35 mm
D	Electroplated	6 g x 25 mm
E	Passivated electroplated	6 g x 25 mm

Fasteners were inserted at 60 mm centres to prevent the MgO board from splitting. Fasteners were inserted parallel to the board surface in one strip of each board so that all of the thread was in contact with the board. In the second strip, fasteners were inserted perpendicular to the sample surface as would be typical installation practice (Figure 2).

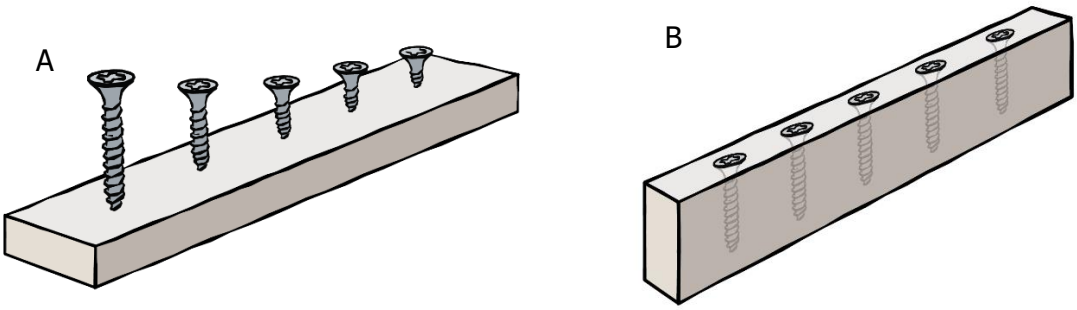

Figure 2. Screws inserted perpendicular (A) and parallel (B) to the sample surface.

All samples were placed in an environmental chamber at 30°C and 90% RH for 90 days and visually inspected at regular intervals. At the end of the test period, fasteners were removed from the strips of MgO board and visually inspected to assess the extent of any visible corrosion.

4. Results and discussion

4.1 Composition analysis

The results of XRF analysis for the MgO boards are shown in Table 3 and Table 4. Results are presented as the percentage (%) of total sample mass. Results shown in Table 3 were determined using the fused bead method. Chlorine (Cl) and sulphur (S) were not detected using the fused bead method but were detected using the pressed powder method and are shown in Table 4.

Table 3. Chemical composition and loss on ignition (LOI) of each board obtained by XRF fused bead method (wt %).

	MgO1	MgO2	MgO3	MgO4
Fe_2O_3	0.29	0.36	0.32	0.31
MnO	0.02	0.02	0.02	0.02
TiO_2	0.07	0.05	0.02	0.02
CaO	2.85	2.88	1.56	1.34
K_2O	0.08	0.18	0.17	0.10
SO_3	1.74	1.87	0.83	0.59
P_2O_5	0.04	0.05	0.04	0.03
SiO_2	6.91	10.15	7.08	7.63
Al_2O_3	0.87	1.09	0.84	0.95
MgO	46.37	41.83	48.78	47.20
Na_2O	0.16	0.40	0.29	0.24
LOI	40.57	41.09	40.05	41.56

Table 4. Composition of chlorine and sulphur of each board obtained by XRF pressed powder method (wt %).

	MgO1	MgO2	MgO3	MgO4
Chlorine	0.04	0.073	10.32	9.76
Sulphur	4.19	4.76	0.23	0.20

Compositional analysis by XRF showed differences in the chemical composition of the four MgO samples. XRF shows that the boards contain 42–49% MgO. The loss on ignition for each board is 40–42%, which is likely related to the wood-fibre content of each board. Subtle differences exist between the quantities of other elements. Of note are the differences in chlorine and sulphur content across the four samples. MgO1 and MgO2 contained negligible chlorine, whereas MgO3 and MgO4 contained a significant amount by comparison. The level of chlorine content in MgO3 and MgO4 is like that found by Aiken, Russell et al. (2020) in their study of magnesium oxychloride boards. Therefore, it would be reasonable to assume that MgO3 and MgO4 contain an oxychloride cement. The low chlorine content and higher sulphur content in MgO1 and MgO2 suggests that those boards are not based on oxychloride cement and may instead have a magnesium oxysulphate binder. Further elemental analysis would be required to confirm these findings.

4.2 Modulus of rupture

Figure 3 shows the ratio of the wet condition MOR of the tested specimens after soaking in water at ambient temperature for 24 hours compared with the corresponding MOR of reference control specimens. Clause 6.1 of AS/NZS 2908.2:2000 requires that the mean MOR under wet conditions shall not be less than 50% of the mean MOR under equilibrium conditions (denoted by the red dashed line). All MgO samples retained over 90% of their equilibrium condition strength in the wet condition.

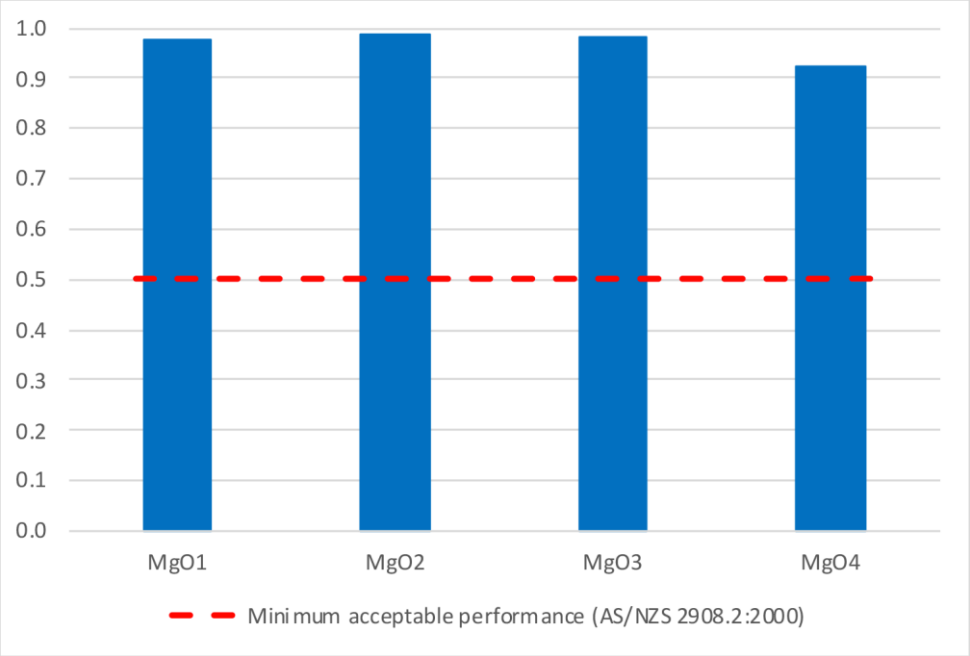

Figure 3. Ratio of the wet condition MOR compared with the corresponding MOR of reference control samples. The red line denotes the minimum acceptable ratio according to AS/NZS 2908.2:2000.

4.3 Frost resistance

Figure 4 shows the ratio of the wet condition MOR of tested specimens after 50 freeze-thaw cycles compared with the corresponding MOR of reference control specimens. Freeze-thaw testing assesses the susceptibility of failure due to dilative pressure exerted internally when water-filled pores within cellulose fibre-cement sheets freeze. According to AS/NZS 2908.2:2000, the ratio of wet to control MOR must exceed 0.75 to be deemed acceptable. MgO1 and MgO2 exceeded the 0.75 requirement with ratios of 0.89 and 0.93 respectively. MgO3 and MgO4 had ratios of 0.38 and 0.46 respectively, which did not meet the 0.75 performance requirement of AS/NZS 2908.2:2000.

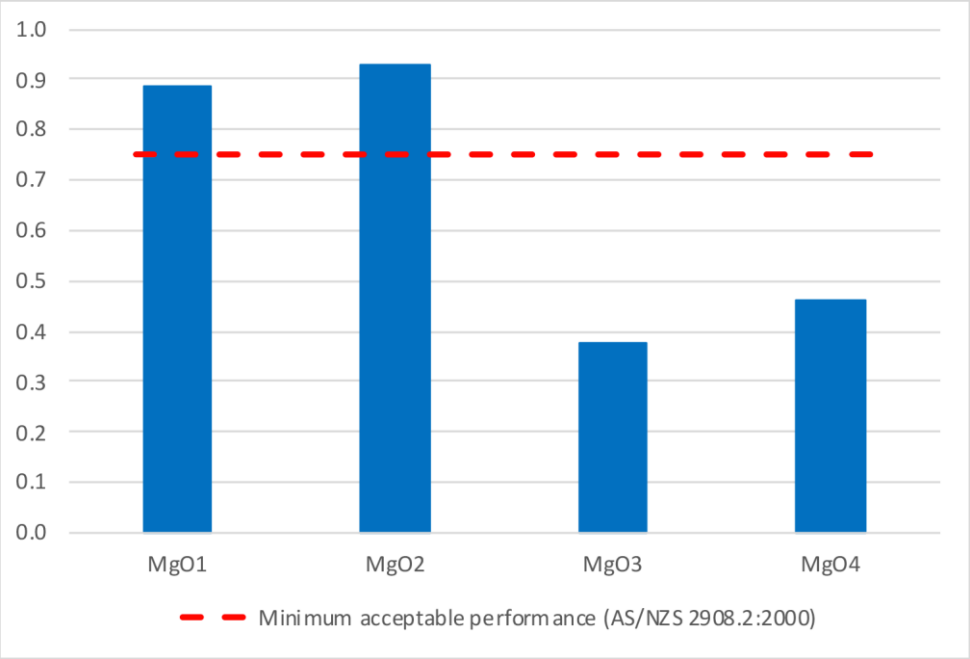

Figure 4. Ratio of the wet condition MOR after 50 freeze-thaw cycles compared with the corresponding MOR of reference control specimens. The red line denotes the minimum acceptable ratio according to AS/NZS 2908.2:2000.

Colour changes were observed in MgO1, which changed from white to yellow/brown. No major changes were observed in other samples as a result of frost resistance testing.

4.4 Warm water immersion

Figure 5 shows the ratio of the wet condition MOR of tested specimens after immersion in warm water compared with the corresponding MOR of reference control specimens. According to AS/NZS 2908.2:2000, the ratio of wet to control MOR must exceed 0.75 to be deemed acceptable. All MgO samples failed to meet the acceptance requirement. Bending strength was reduced by at least 50% in all MgO samples following the prolonged warm water immersion.

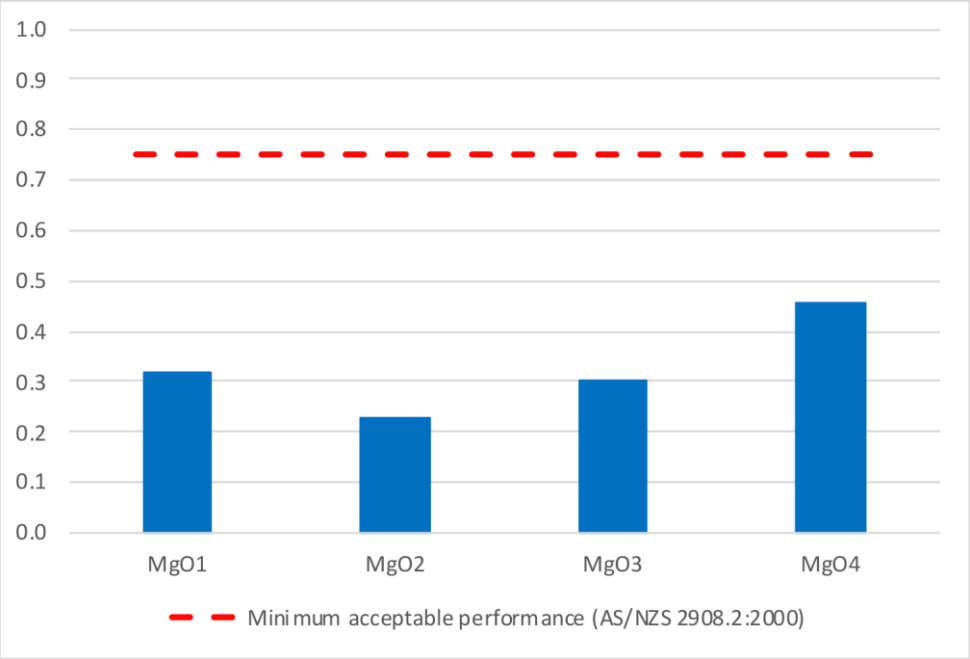

Figure 5. Ratio of wet condition MOR after warm water immersion compared with the corresponding MOR of reference control specimens. The red line denotes the minimum acceptable ratio according to AS/NZS 2908.2:2000.

Although no specific analysis was done to investigate the cause of strength reduction following the warm water immersion, visual observations of the MgO samples provide some information as to potential means of degradation. Compared to control samples, boards that had been immersed in warm water went from white to a grey or yellow/brown colour. The colour change was slight in the case of MgO1 and MgO3 and more obvious in MgO2 and MgO4. The reinforcing mesh component remained intact in all samples except MgO2 where it delaminated from the cement matrix entirely after the test.

4.5 Soak-dry

Figure 6 shows the ratio of the wet condition MOR of tested specimens after 25 soak-dry cycles compared with the corresponding MOR of reference control specimens. According to AS/NZS 2908.2:2000, the ratio of wet to control MOR must exceed 0.75 to be deemed acceptable. MgO1 and MgO2 both had ratios of 0.93 and exceeded the performance requirement. MgO3 and MgO4 had ratios of 0.43 and 0.47 respectively and did not meet the performance level required.

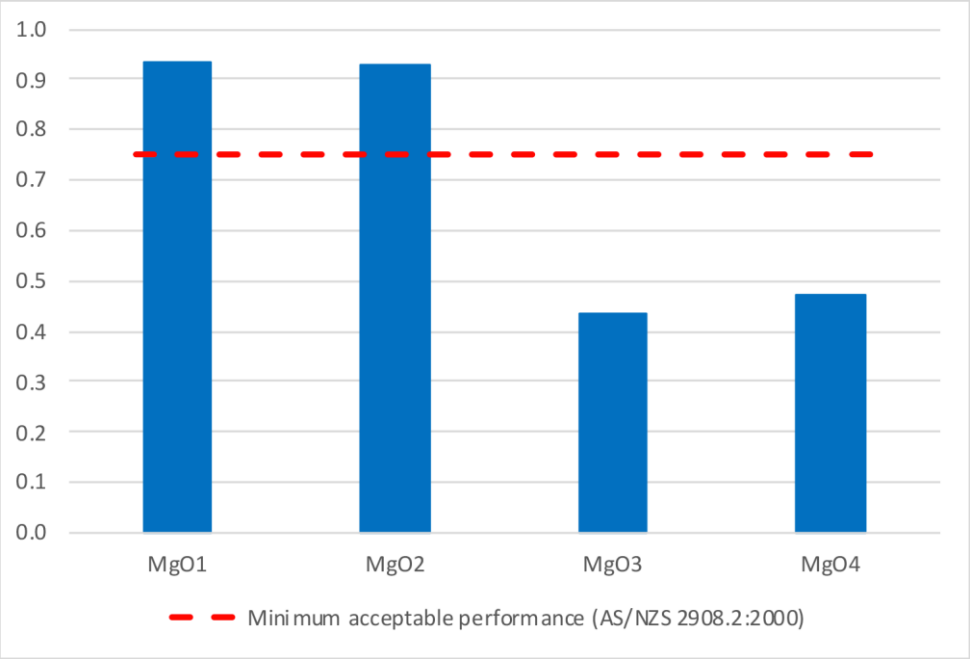

Figure 6. Ratio of the wet condition MOR after 25 soak-dry cycles compared with the corresponding MOR of reference control specimens. The red line denotes the minimum acceptable ratio according to AS/NZS 2908.2:2000.

Visual observations included slight colour change in MgO2, which changed from white to a non-uninform light-brown appearance. No major changes were noted in other samples.

4.6 Water vapour transmission

Table 5 shows the results of water vapour transmission testing. MgO1 and MgO2 showed the greatest resistance to water vapour transmission of all samples tested, with results of 1.26 and 1.21 MNs/g respectively. MgO3 showed the lowest resistance (0.65 MNs/g).

Table 5. Water vapour transmission properties of tested samples.

Sample ID	Mean vapour flow rate (g/m²d)	Mean vapour flow resistance (MNs/g)
MgO1	88.20	1.26
MgO2	91.18	1.21
MgO3	169.79	0.65
MgO4	149.80	0.82

4.7 Water absorption

Table 6 shows the mass gained by each sample following 48 hours of soaking. This test is used as a routine test to determine the tendency of a product to absorb water and determine uniformity of the product. The results show that the mass of MgO samples increased 27–39% after 48 hours of soaking.

Table 6. Mass gain of samples following water absorption tests.

Sample ID	Mass gain (%)
MgO1	31.6 ± 1.1
MgO2	39.4 ± 3.2
MgO3	31.0 ± 1.0
MgO4	26.9 ± 2.7

4.8 Performance in a high-humidity environment

Figure 7 shows the ratio of the MOR of tested specimens following 90 days at 30°C and 90% RH compared with the corresponding MOR of wet control specimens. This test is included in PAS 670:2021 and includes the requirement that no liquid droplets shall appear on the surface of the boards and that the strength retention between humid tested boards and control samples shall be greater than or equal to 75% (denoted by the red line in Figure 7).

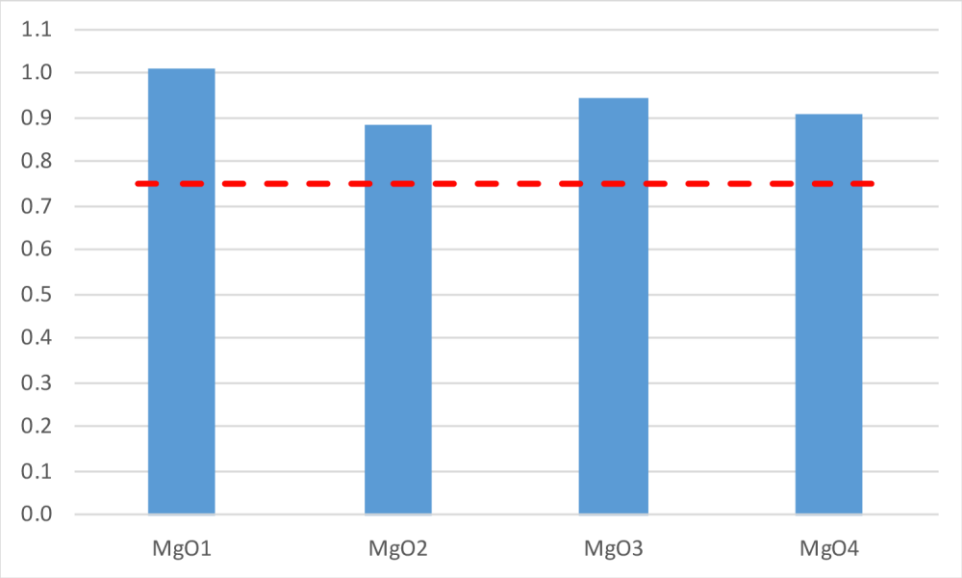

Figure 7. Ratio of humid tested MOR after high-humidity test, compared to MOR of control specimens. The red line denotes the minimum acceptable ratio according to PAS 670:2021.

The results show that all MgO samples retained at least 80% of their original bending strength after 90 days of exposure. Compared to Aiken, McPolin et al. (2020) and Wøhler Neilsen et al. (2019), who found that both MOS and MOC boards displayed 'crying' droplets at exposure to similarly high relative humidity conditions, no visible water droplets were observed on the surface of any boards during the 90 days in this study. It is possible that this is due to the nature of the boards selected in this study. However, there may also have been limitations with the test set-up as compared with Aiken, McPolin et al. (2020) and Wøhler Neilsen et al. (2019). It could be that the air movement inside the climate chamber was sufficient to cause evaporation of any water droplets before they could be observed. In addition, the vertical orientation of samples may have prevented any water droplets from being maintained on the sample surface.

4.9 Fastener corrosion

The resulting levels of corrosion for the different fastener types and for different boards are summarised in Table 7 and shown in Figure 8. The results show that MgO3 and MgO4 are more corrosive than MgO1 and MgO2 for all fasteners other than 316 and 304 stainless steel types. MgO3 and MgO4 have a higher concentration of chloride and are associated with more severe corrosion of mechanically plated, electroplated and passivated electroplated fasteners. These findings agree with those of Jays et al. (2019) who found that chloride concentration correlates with corrosion. In addition, several others have found that corrosion associated with MgO boards correlated with the presence of magnesium oxychloride cement (Rode et al., 2017; Hansen, Bunch-Nielsen, Grelk & Rode, 2016). Electroplated fasteners (D and E) corroded severely in MgO3 and MgO4. However, they did not corrode in MgO1 and MgO2.

Table 7. Description of visible corrosion of screws in MgO boards.

	Board sample	Screw sample (type)				
		A (316 stainless)	B (304 stainless)	C (mechanically plated)	D (electroplated)	E (passivated electroplated
Parallel to surface	MgO1	-	-	-	-	-
	MgO2	-	-	-	-	-
	MgO3	-	-	Mild corrosion	Severe corrosion	Severe corrosion
	MgO4	-	-	Mild corrosion	Severe corrosion	Severe corrosion
Perpendicular to surface	MgO1	-	-	-	-	-
	MgO2	-	-	-	-	-
	MgO3	-	-	Severe corrosion	Severe corrosion	Severe corrosion
	MgO4	-	-	Severe corrosion	Severe corrosion	Severe corrosion

- = 0–10% surface coverage of corrosion products, mild corrosion = 10–50% surface coverage of corrosion products, severe corrosion = 50–100% surface coverage of corrosion products.

Figure 8. Conditions of screws attached to samples parallel to the sample surface (A) 316 stainless steel, (B) 304 stainless steel, (C) mechanically plated, (D) electroplated, (E) passivated electroplated.

5. Conclusions

Testing and analysis has provided data on the performance of four different MgO boards within a New Zealand context. This has been carried out to evaluate any potential variations in the chemical and physical properties between the different MgO boards.

Tests were primarily based on the methods included in AS/NZS 2908.2:2000, which are commonly used to assess the suitability of fibre-cement sheets for use in New Zealand – a product for which MgO boards are typically used as an alternative. Additional tests were included that had been used in similar research on the performance of MgO boards in both the UK and Australia to enable comparisons with those findings.

MgO board samples were sourced without a detailed knowledge of their chemical composition. However, compositional analysis identified two subsets of board based on differences in chloride concentration. In some cases – for example, after freeze-thaw, soak-dry and water vapour transmission tests – results showed significant differences between boards with different chloride concentrations. In other tests, MgO boards performed similarly or differences did not appear to be associated with chloride concentration. Boards with a higher chloride content were associated with corrosion of mechanically plated, electroplated and passivated electroplated fasteners under the conditions tested, whereas boards with low chloride concentration did not corrode the same fasteners. In addition, differences between boards were apparent from visual observation following the warm water soak test, where delamination of the fibre mesh and partial degradation of the cement component occurred in some cases and not in others.

Overall, the findings from this study show that there is performance variability between MgO boards from different suppliers and that not all boards perform equally in all exposure conditions. These findings highlight the importance of considering the likely in-service conditions when assessing the suitability of a given MgO board for a given application.

References

Aiken, T. A., McPolin, D., Russell, M., Madden, M. & Bagnall, L. (2020). Physical and mechanical performance of magnesium-based construction boards: A comparative study. *Construction and Building Materials*, *270*, 121397. https://doi.org/10.1016/j.conbuildmat.2020.121397

Aiken, T. A., Russell, M., McPolin, D. & Bagnall, L. (2020). Magnesium oxychloride boards: understanding a novel building material. *Materials and Structures*, *53*(5), 1–16. https://doi.org/10.1617/s11527-020-01547-z

Hansen, K. K., Bunch-Nielsen, T., Grelk, B. & Rode, C. (2016). Magnesium-oxide boards cause moisture damage inside facades in new Danish buildings. Paper presented at *International RILEM Conference on Materials, Systems and Structures in Civil Engineering*, Kongens Lyngby, Denmark, 15–29 August.

Jays, N., Olofinjana, A. & Young, D. J. (2019). Assessing variability in the hygrothermal performance of magnesium oxide (MgO) cladding products of the Australian market. *Construction and Building Materials*, *203*, 491–500. https://doi.org/10.1016/j.conbuildmat.2019.01.111

Rode, C., Bunch-Nielsen, T., Hansen, K. K. & Grelk, B. (2017). Moisture damage with magnesium oxide boards in Danish facade structures. *Energy Procedia*, *132*, 765–770. https://doi.org/10.1016/j.egypro.2017.10.025

Walling, S. A. & Provis, J. L. (2016). Magnesia-based cements: A journey of 150 years, and cements for the future? *Chemical Reviews*, *116*(7), 4170–4204. https://doi.org/10.1021/acs.chemrev.5b00463

Wang, L., Chen, S. S., Tsang, D. C., Poon, C. -S. & Shih, K. (2016). Recycling contaminated wood into eco-friendly particleboard using green cement and carbon dioxide curing. *Journal of Cleaner Production*, *137*, 861–870. https://doi.org/10.1016/j.jclepro.2016.07.180

Wøhler Nielsen, S., Rode, C., Bunch-Nielsen, T., Hansen, K., Kunther, W. & Grelk, B. (2019). Properties of magnesium oxide boards used as sheathing in exterior walls. *MATEC Web of Conferences*, *282*, 02019. https://doi.org/10.1051/matecconf/201928202091

Appendix A

Bending strength

MgO-1 Controls							
Sample	Parallel samples MOR (MPa)		Perpendicular samples MOR (MPa)		Mean R_{fci} (MPa)	Mean R_{fi} (MPa)	$r_i = R_{fi}/R_{fci}$
	Control MOR (MPa) R_{fci}	Specimen MOR (MPa) R_{fi}	Control MOR (MPa) R_{fci}	Specimen MOR (MPa) R_{fi}			
MgO-1-1	9.2	8.6	8.6	8.7	8.9	8.7	0.97
MgO-1-2	11.2	10.2	8.6	7.9	9.9	9.1	0.92
MgO-1-3	12.2	13.9	9.5	11.7	10.9	12.8	1.18
MgO-1-4	12.8	13.5	9.5	9.8	11.1	11.7	1.05
MgO-1-5	9.3	8.9	7.8	7.6	8.6	8.3	0.96
MgO-1-6	9.2	8.9	7.6	7.5	8.4	8.2	0.98
MgO-1-7	11.7	12.1	8.5	10.7	10.1	11.4	1.13
MgO-1-8	12.7	13.2	9.9	11.4	11.3	12.3	1.09
MgO-1-9	9.5	9.4	8.1	8.0	8.8	8.7	0.99
MgO-1-10	9.7	8.9	8.4	9.0	9.0	9.0	0.99
Mean ratio, r							1.03
Standard Deviation, s							0.08
Lower 95% Confidence limit L_i=r-0.58s							0.98

MgO-2 Controls							
Sample	Parallel samples MOR (MPa)		Perpendicular samples MOR (MPa)		Mean R_{fci} (MPa)	Mean R_{fi} (MPa)	$r_i = R_{fi}/R_{fci}$
	Control MOR (MPa) R_{fci}	Specimen MOR (MPa) R_{fi}	Control MOR (MPa) R_{fci}	Specimen MOR (MPa) R_{fi}			
MgO-2-1	9.0	7.7	6.9	5.5	8.0	6.6	0.83
MgO-2-2	9.3	9.4	8.6	9.8	9.0	9.6	1.08
MgO-2-3	9.0	9.9	7.0	9.2	8.0	9.6	1.20
MgO-2-4	8.9	10.2	7.1	8.6	8.0	9.4	1.17
MgO-2-5	9.2	8.2	7.4	5.3	8.3	6.8	0.82
MgO-2-6	9.5	9.4	9.0	11.3	9.3	10.4	1.12
MgO-2-7	10.5	11.8	8.2	10.6	9.3	11.2	1.20
MgO-2-8	11.8	13.1	10.6	12.3	11.2	12.7	1.13
MgO-2-9	8.7	12.6	9.2	11.2	9.0	11.9	1.33
MgO-2-10	13.1	11.6	10.3	11.1	11.7	11.3	0.97
Mean ratio, r							1.08
Standard Deviation, s							0.17
Lower 95% Confidence limit L_i=r-0.58s							0.99

MgO3 Controls							
Sample	Parallel samples MOR (MPa)		Perpendicular samples MOR (MPa)		Mean R_{fci} (MPa)	Mean R_{fi} (MPa)	$r_i = R_{fi}/R_{fci}$
	Control MOR (MPa) R_{fci}	Specimen MOR (MPa) R_{fi}	Control MOR (MPa) R_{fci}	Specimen MOR (MPa) R_{fi}			
MgO3-1	16.3	16.0	13.7	12.8	15.0	14.4	0.96
MgO3-2	15.3	16.0	12.2	12.9	13.7	14.4	1.05
MgO3-3	18.8	18.7	19.1	18.6	18.9	18.6	0.98
MgO3-4	17.6	19.4	17.9	19.7	17.8	19.6	1.10
MgO3-5	14.8	15.2	12.0	12.1	13.4	13.6	1.02
MgO3-6	15.5	13.8	13.2	12.6	14.4	13.2	0.92
MgO3-7	17.0	19.1	16.9	17.0	16.9	18.0	1.06
MgO3-8	17.6	19.0	18.6	19.7	18.1	19.4	1.07
MgO3-9	14.8	15.3	11.0	10.5	12.9	12.9	1.00
MgO3-10	14.9	14.5	11.6	10.9	13.2	12.7	0.96
Mean ratio, r							1.01
Standard Deviation, s							0.06
Lower 95% Confidence limit L_i=r-0.58s							0.98

MgO4 Controls							
Sample	Parallel samples MOR (MPa)		Perpendicular samples MOR (MPa)		Mean R_{fci} (MPa)	Mean R_{fi} (MPa)	$r_i = R_{fi}/R_{fci}$
	Control MOR (MPa) R_{fci}	Specimen MOR (MPa) R_{fi}	Control MOR (MPa) R_{fci}	Specimen MOR (MPa) R_{fi}			
MgO4-1	10.1	9.0	11.3	11.6	10.7	10.3	0.96
MgO4-2	9.4	7.7	11.1	11.3	10.3	9.5	0.92
MgO4-3	13.1	12.2	13.3	15.2	13.2	13.7	1.04
MgO4-4	12.9	11.9	13.1	14.7	13.0	13.3	1.02
MgO4-5	10.1	8.3	10.9	10.1	10.5	9.2	0.88
MgO4-6	8.6	6.9	10.2	10.1	9.4	8.5	0.90
MgO4-7	14.2	13.7	13.3	15.1	13.7	14.4	1.05
MgO4-8	14.2	10.0	14.1	15.1	14.2	12.6	0.89
MgO4-9	9.7	8.4	10.8	10.5	10.2	9.5	0.92
MgO4-10	9.2	10.2	11.2	11.4	10.2	10.8	1.06
Mean ratio, r							0.96
Standard Deviation, s							0.07
Lower 95% Confidence limit Li=r-0.58s							0.92

Frost resistance

MgO1 Freeze-Thaw							
Sample	Parallel samples MOR (MPa)		Perpendicular samples MOR (MPa)		Mean R_{fci} (MPa)	Mean R_{fi} (MPa)	$r_i = R_{fi}/R_{fci}$
	Control MOR (MPa) R_{fci}	Specimen MOR (MPa) R_{fi}	Control MOR (MPa) R_{fci}	Specimen MOR (MPa) R_{fi}			
MgO-1-1	8.6	8.7	8.7	6.8	8.7	7.7	0.89
MgO-1-2	10.2	10.7	7.9	7.0	9.1	8.9	0.98
MgO-1-3	13.9	13.7	11.7	9.6	12.8	11.7	0.91
MgO-1-4	13.5	13.8	9.8	10.1	11.7	11.9	1.02
MgO-1-5	8.9	7.8	7.6	6.5	8.3	7.1	0.86
MgO-1-6	8.9	8.6	7.5	6.3	8.2	7.5	0.91
MgO-1-7	12.1	13.2	10.7	9.1	11.4	11.1	0.98
MgO-1-8	13.2	12.7	11.4	10.5	12.3	11.6	0.94
MgO-1-9	9.4	8.8	8.0	6.6	8.7	7.7	0.88
MgO-1-10	8.9	7.6	9.0	7.2	9.0	7.4	0.82
Mean ratio, r							0.92
Standard Deviation, s							0.06
Lower 95% Confidence limit Li=r-0.58s							0.89

MgO2 Freeze-Thaw							
Sample	Parallel samples MOR (MPa)		Perpendicular samples MOR (MPa)		Mean R_{fci} (MPa)	Mean R_{fi} (MPa)	$r_i = R_{fi}/R_{fci}$
	Control MOR (MPa) R_{fci}	Specimen MOR (MPa) R_{fi}	Control MOR (MPa) R_{fci}	Specimen MOR (MPa) R_{fi}			
MgO-2-1	7.7	7.2	5.5	5.0	6.6	6.1	0.93
MgO-2-2	9.4	9.0	9.8	10.0	9.6	9.5	0.99
MgO-2-3	9.9	10.2	9.2	8.5	9.6	9.4	0.98
MgO-2-4	10.2	11.5	8.6	9.6	9.4	10.5	1.12
MgO-2-5	8.2	8.3	5.3	4.7	6.8	6.5	0.96
MgO-2-6	9.4	8.5	11.3	9.1	10.4	8.8	0.85
MgO-2-7	11.8	11.9	10.6	10.8	11.2	11.4	1.02
MgO-2-8	13.1	13.8	12.3	12.7	12.7	13.2	1.04
MgO-2-9	12.6	12.1	11.2	8.4	11.9	10.3	0.86
MgO-2-10	11.6	12.8	11.1	11.6	11.3	12.2	1.08
Mean ratio, r							0.98
Standard Deviation, s							0.09
Lower 95% Confidence limit L_i=r-0.58s							0.93

MgO3 Freeze-Thaw							
Sample	Parallel samples MOR (MPa)		Perpendicular samples MOR (MPa)		Mean R_{fci} (MPa)	Mean R_{fi} (MPa)	$r_i = R_{fi}/R_{fci}$
	Control MOR (MPa) R_{fci}	Specimen MOR (MPa) R_{fi}	Control MOR (MPa) R_{fci}	Specimen MOR (MPa) R_{fi}			
MgO3-1	16.0	6.5	12.8	6.7	14.4	6.6	0.46
MgO3-2	16.0	5.6	12.9	5.3	14.4	5.5	0.38
MgO3-3	18.7	16.8	18.6	12.7	18.6	14.8	0.79
MgO3-4	19.4	9.3	19.7	7.7	19.6	8.5	0.44
MgO3-5	15.2	5.7	12.1	5.0	13.6	5.4	0.39
MgO3-6	13.8	5.6	12.6	5.8	13.2	5.7	0.43
MgO3-7	19.1	7.0	17.0	5.4	18.0	6.2	0.35
MgO3-8	19.0	6.4	19.7	6.8	19.4	6.6	0.34
MgO3-9	15.3	5.2	10.5	4.9	12.9	5.1	0.39
MgO3-10	14.5	9.9	10.9	10.1	12.7	10.0	0.79
Mean ratio, r							0.48
Standard Deviation, s							0.17
Lower 95% Confidence limit Li=r-0.58s							0.38

MgO4 Freeze-Thaw							
Sample	Parallel samples MOR (MPa)		Perpendicular samples MOR (MPa)		Mean R_{fci} (MPa)	Mean R_{fi} (MPa)	$r_i = R_{fi}/R_{fci}$
	Control MOR (MPa) R_{fci}	Specimen MOR (MPa) R_{fi}	Control MOR (MPa) R_{fci}	Specimen MOR (MPa) R_{fi}			
MgO4-1	9.0	4.5	11.6	4.8	10.3	4.7	0.46
MgO4-2	7.7	4.2	11.3	4.5	9.5	4.3	0.45
MgO4-3	12.2	7.2	15.2	7.1	13.7	7.1	0.52
MgO4-4	11.9	5.8	14.7	6.3	13.3	6.0	0.45
MgO4-5	8.3	4.4	10.1	4.2	9.2	4.3	0.47
MgO4-6	6.9	4.1	10.1	4.7	8.5	4.4	0.52
MgO4-7	13.7	7.0	15.1	7.1	14.4	7.1	0.49
MgO4-8	10.0	5.5	15.1	5.9	12.6	5.7	0.45
MgO4-9	8.4	4.7	10.5	5.1	9.5	4.9	0.52
MgO4-10	10.2	4.4	11.4	5.5	10.8	4.9	0.46
Mean ratio, r							0.48
Standard Deviation, s							0.03
Lower 95% Confidence limit Li=r-0.58s							0.46

Warm water immersion

MgO1 Warm water Immersion							
Sample	Parallel samples MOR (MPa)		Perpendicular samples MOR (MPa)		Mean R_{fci} (MPa)	Mean R_{fi} (MPa)	$r_i = R_{fi}/R_{fci}$
	Control MOR (MPa) R_{fci}	Specimen MOR (MPa) R_{fi}	Control MOR (MPa) R_{fci}	Specimen MOR (MPa) R_{fi}			
MgO-1-1	8.6	3.9	8.7	2.5	8.7	3.2	0.37
MgO-1-2	10.2	3.6	7.9	4.1	9.1	3.9	0.43
MgO-1-3	13.9	5.6	11.7	2.8	12.8	4.2	0.33
MgO-1-4	13.5	4.6	9.8	4.9	11.7	4.8	0.41
MgO-1-5	8.9	2.7	7.6	1.2	8.3	2.0	0.24
MgO-1-6	8.9	2.0	7.5	3.1	8.2	2.5	0.31
MgO-1-7	12.1	5.2	10.7	4.0	11.4	4.6	0.40
MgO-1-8	13.2	4.7	11.4	5.2	12.3	4.9	0.40
MgO-1-9	9.4	3.1	8.0	1.7	8.7	2.4	0.28
MgO-1-10	8.9	2.8	9.0	3.6	9.0	3.2	0.36
Mean ratio, r							0.35
Standard Deviation, s							0.06
Lower 95% Confidence limit Li=r-0.58s							0.32

MgO2 Warm water Immersion							
Sample	Parallel samples MOR (MPa)		Perpendicular samples MOR (MPa)		Mean R_{fci} (MPa)	Mean R_{fi} (MPa)	$r_i = R_{fi}/R_{fci}$
	Control MOR (MPa) R_{fci}	Specimen MOR (MPa) R_{fi}	Control MOR (MPa) R_{fci}	Specimen MOR (MPa) R_{fi}			
MgO-2-1	7.7	2.7	5.5	1.6	6.6	2.1	0.32
MgO-2-2	9.4	2.0	9.8	2.4	9.6	2.2	0.23
MgO-2-3	9.9	3.2	9.2	0.9	9.6	2.0	0.21
MgO-2-4	10.2	1.0	8.6	4.2	9.4	2.6	0.27
MgO-2-5	8.2	3.0	5.3	1.9	6.8	2.5	0.36
MgO-2-6	9.4	2.0	11.3	3.7	10.4	2.9	0.28
MgO-2-7	11.8	4.1	10.6	1.1	11.2	2.6	0.23
MgO-2-8	13.1	1.1	12.3	4.5	12.7	2.8	0.22
MgO-2-9	12.6	2.9	11.2	1.8	11.9	2.4	0.20
MgO-2-10	11.6	2.6	11.1	3.9	11.3	3.2	0.29
Mean ratio, r							0.26
Standard Deviation, s							0.05
Lower 95% Confidence limit Li=r-0.58s							0.23

MgO3 Warm water Immersion							
Sample	Parallel samples MOR (MPa)		Perpendicular samples MOR (MPa)		Mean R_{fci} (MPa)	Mean R_{fi} (MPa)	$r_i = R_{fi}/R_{fci}$
	Control MOR (MPa) R_{fci}	Specimen MOR (MPa) R_{fi}	Control MOR (MPa) R_{fci}	Specimen MOR (MPa) R_{fi}			
MgO3-1	16.0	4.0	12.8	5.5	14.4	4.8	0.33
MgO3-2	16.0	3.6	12.9	5.0	14.4	4.3	0.30
MgO3-3	18.7	7.0	18.6	7.4	18.6	7.2	0.39
MgO3-4	19.4	6.3	19.7	7.7	19.6	7.0	0.36
MgO3-5	15.2	3.7	12.1	4.7	13.6	4.2	0.31
MgO3-6	13.8	3.5	12.6	5.0	13.2	4.2	0.32
MgO3-7	19.1	5.7	17.0	5.5	18.0	5.6	0.31
MgO3-8	19.0	5.7	19.7	5.9	19.4	5.8	0.30
MgO3-9	15.3	3.6	10.5	4.3	12.9	3.9	0.31
MgO3-10	14.5	3.1	10.9	4.5	12.7	3.8	0.30
Mean ratio, r							0.32
Standard Deviation, s							0.03
Lower 95% Confidence limit Li=r-0.58s							0.30

MgO4 Warm water Immersion							
Sample	Parallel samples MOR (MPa)		Perpendicular samples MOR (MPa)		Mean R_{fci} (MPa)	Mean R_{fi} (MPa)	$r_i = R_{fi}/R_{fci}$
	Control MOR (MPa) R_{fci}	Specimen MOR (MPa) R_{fi}	Control MOR (MPa) R_{fci}	Specimen MOR (MPa) R_{fi}			
MgO4-1	9.0	4.6	11.6	4.9	10.3	4.8	0.47
MgO4-2	7.7	4.2	11.3	5.0	9.5	4.6	0.48
MgO4-3	12.2	5.2	15.2	5.6	13.7	5.4	0.40
MgO4-4	11.9	5.2	14.7	6.4	13.3	5.8	0.43
MgO4-5	8.3	4.7	10.1	4.7	9.2	4.7	0.51
MgO4-6	6.9	4.7	10.1	4.7	8.5	4.7	0.55
MgO4-7	13.7	6.6	15.1	6.8	14.4	6.7	0.47
MgO4-8	10.0	6.1	15.1	7.0	12.6	6.5	0.52
MgO4-9	8.4	5.9	10.5	5.0	9.5	5.5	0.58
MgO4-10	10.2	5.8	11.4	4.9	10.8	5.4	0.49
Mean ratio, r							0.49
Standard Deviation, s							0.05
Lower 95% Confidence limit Li=r-0.58s							0.46

Soak-dry

MgO1 Soak-Dry							
Sample	Parallel samples MOR (MPa)		Perpendicular samples MOR (MPa)		Mean R_{fci} (MPa)	Mean R_{fi} (MPa)	$r_i = R_{fi}/R_{fci}$
	Control MOR (MPa) R_{fci}	Specimen MOR (MPa) R_{fi}	Control MOR (MPa) R_{fci}	Specimen MOR (MPa) R_{fi}			
MgO-1-1	8.6	8.2	8.7	7.1	8.7	7.6	0.88
MgO-1-2	10.2	9.1	7.9	8.0	9.1	8.5	0.94
MgO-1-3	13.9	13.5	11.7	10.4	12.8	12.0	0.93
MgO-1-4	13.5	12.4	9.8	10.8	11.7	11.6	1.00
MgO-1-5	8.9	9.2	7.6	6.9	8.3	8.1	0.98
MgO-1-6	8.9	7.6	7.5	7.6	8.2	7.6	0.92
MgO-1-7	12.1	12.0	10.7	9.6	11.4	10.8	0.95
MgO-1-8	13.2	11.9	11.4	11.2	12.3	11.6	0.94
MgO-1-9	9.4	9.7	8.0	8.3	8.7	9.0	1.04
MgO-1-10	8.9	9.2	9.0	8.6	9.0	8.9	0.99
Mean ratio, r							0.96
Standard Deviation, s							0.04
Lower 95% Confidence limit Li=r-0.58s							0.93

MgO2 Soak-Dry							
Sample	Parallel samples MOR (MPa)		Perpendicular samples MOR (MPa)		Mean R_{fci} (MPa)	Mean R_{fi} (MPa)	$r_i = R_{fi}/R_{fci}$
	Control MOR (MPa) R_{fci}	Specimen MOR (MPa) R_{fi}	Control MOR (MPa) R_{fci}	Specimen MOR (MPa) R_{fi}			
MgO-2-1	7.7	8.9	5.5	5.4	6.6	7.2	1.09
MgO-2-2	9.4	8.5	9.8	9.9	9.6	9.2	0.95
MgO-2-3	9.9	9.8	9.2	7.9	9.6	8.8	0.92
MgO-2-4	10.2	9.9	8.6	9.5	9.4	9.7	1.03
MgO-2-5	8.2	9.5	5.3	5.2	6.8	7.4	1.09
MgO-2-6	9.4	8.3	11.3	10.1	10.4	9.2	0.89
MgO-2-7	11.8	11.0	10.6	9.7	11.2	10.3	0.92
MgO-2-8	13.1	12.8	12.3	12.4	12.7	12.6	0.99
MgO-2-9	12.6	11.8	11.2	9.2	11.9	10.5	0.88
MgO-2-10	11.6	11.6	11.1	10.6	11.3	11.1	0.98
Mean ratio, r							0.97
Standard Deviation, s							0.08
Lower 95% Confidence limit Li=r-0.58s							0.93

MgO3 Soak-Dry							
Sample	Parallel samples MOR (MPa)		Perpendicular samples MOR (MPa)		Mean R_{fci} (MPa)	Mean R_{fi} (MPa)	$r_i = R_{fi}/R_{fci}$
	Control MOR (MPa) R_{fci}	Specimen MOR (MPa) R_{fi}	Control MOR (MPa) R_{fci}	Specimen MOR (MPa) R_{fi}			
MgO3-1	16.0	9.4	12.8	7.4	14.4	8.4	0.59
MgO3-2	16.0	6.0	12.9	6.0	14.4	6.0	0.41
MgO3-3	18.7	14.5	18.6	14.5	18.6	14.5	0.78
MgO3-4	19.4	8.4	19.7	9.6	19.6	9.0	0.46
MgO3-5	15.2	6.3	12.1	6.0	13.6	6.1	0.45
MgO3-6	13.8	6.4	12.6	8.5	13.2	7.4	0.56
MgO3-7	19.1	7.3	17.0	6.9	18.0	7.1	0.39
MgO3-8	19.0	6.9	19.7	7.9	19.4	7.4	0.38
MgO3-9	15.3	6.1	10.5	5.8	12.9	6.0	0.46
MgO3-10	14.5	6.0	10.9	7.5	12.7	6.7	0.53
Mean ratio, r							0.50
Standard Deviation, s							0.12
Lower 95% Confidence limit Li=r-0.58s							0.43

MgO4 Soak-Dry							
Sample	Parallel samples MOR (MPa)		Perpendicular samples MOR (MPa)		Mean R_{fci} (MPa)	Mean R_{fi} (MPa)	$r_i = R_{fi}/R_{fci}$
	Control MOR (MPa) R_{fci}	Specimen MOR (MPa) R_{fi}	Control MOR (MPa) R_{fci}	Specimen MOR (MPa) R_{fi}			
MgO4-1	9.0	5.7	11.6	6.2	10.3	5.9	0.58
MgO4-2	7.7	4.5	11.3	4.8	9.5	4.6	0.49
MgO4-3	12.2	6.5	15.2	5.8	13.7	6.1	0.45
MgO4-4	11.9	5.6	14.7	5.8	13.3	5.7	0.43
MgO4-5	8.3	4.3	10.1	4.1	9.2	4.2	0.46
MgO4-6	6.9	4.5	10.1	5.9	8.5	5.2	0.61
MgO4-7	13.7	6.8	15.1	6.6	14.4	6.7	0.46
MgO4-8	10.0	6.2	15.1	7.0	12.6	6.6	0.53
MgO4-9	8.4	5.3	10.5	6.1	9.5	5.7	0.61
MgO4-10	10.2	5.0	11.4	5.8	10.8	5.4	0.50
Mean ratio, r							0.51
Standard Deviation, s							0.07
Lower 95% Confidence limit Li=r-0.58s							0.47

Water vapour transmission

Sample ID	Vapour flow rate (g/m2d)	Mean vapour flow rate (g/m2d)	Resistance (MNs/g)	Mean resistance (MNs/g)
MgO-1	81.42	88.20	1.36	1.26
	94.47		1.16	
MgO-2	91.18	91.18	1.21	1.21
	91.19		1.21	
MgO-3	178.20	169.79	0.62	0.65
	161.38		0.68	
MgO-4	197.75	149.80	0.56	0.82
	101.84		1.08	

High-humidity test

Sample ID	Mean Control MOR (MPa)	Mean Tested MOR (MPa)	Ratio of control to tested MOR
MgO-1	9.70	10.11	1.04
MgO-2	9.16	8.77	0.96
MgO-3	15.43	14.79	0.96
MgO-4	11.55	10.13	0.88